

## Phase Diagram and Orientational Order in a Biaxial Lattice Model: A Monte Carlo Study

F. Biscarini,<sup>1,\*</sup> C. Chiccoli,<sup>2</sup> P. Pasini,<sup>2</sup> F. Semeria,<sup>2</sup> and C. Zannoni<sup>1</sup>

<sup>1</sup>*Dipartimento di Chimica Fisica ed Inorganica, Università di Bologna, Viale Risorgimento 4, 40136 Bologna, Italy*

<sup>2</sup>*Istituto Nazionale di Fisica Nucleare, Sezione di Bologna, Via Irnerio 46, 40126 Bologna, Italy*

(Received 27 March 1995)

We have determined the phase diagram for a lattice system of biaxial particles interacting with a second rank anisotropic potential using Monte Carlo simulations for a number of values of the molecular biaxiality. We find increasing differences from mean field theory as the biaxiality increases. We have also calculated for the first time the full set of second rank biaxial and uniaxial order parameters and their temperature dependence, and on this basis we comment on the difficulties of measuring phase biaxiality by NMR.

PACS numbers: 61.30.Gd, 61.30.Cz, 64.70.Md

Liquid crystal phases formed by biaxial particles have been studied using a number of theoretical methods; e.g., without trying to be exhaustive, mean field theory (MFT) [1–4], counting methods [5], Landau–de Gennes theory [6,7], bifurcation analysis [8], density functional theory [9], etc. All the theories mentioned above predict that the system will exhibit four phases as the molecular biaxiality varies: a positive ( $N_+$ ) and a negative ( $N_-$ ) uniaxial phase, respectively, formed by prolate or oblate particles, a biaxial ( $N_B$ ), and an isotropic ( $I$ ) phase. The nematic-isotropic phase transition is expected to be first order and to weaken as the biaxiality increases until it becomes continuous at the point (Landau bicritical point) of maximum molecular biaxiality. At this point the system should go directly from a biaxial to an isotropic phase. The biaxial-uniaxial transition is expected to be second order. The possibility of a biaxial-nematic mesophase has been confirmed by some computer simulations of a lattice system of biaxial particles [10,11], and of a fluid system of biaxial spherocylinders [12]. On the experimental side, there is an increasing number of biaxial lyotropic [13] and polymeric [14] phases while the observation of thermotropic, claimed by a number of authors [15], typically on the basis of optical observations, is still questioned [16].

Given this extensive activity, it is surprising that a detailed computer experimental study of the phase diagram and, even more, of the full set of order parameters and their detailed temperature dependence within the biaxial and uniaxial phases are not available as yet. This information is crucial for the study of static but also, indirectly, of dynamic properties [17] and in general to validate molecular theories. In this Letter we make an attack on this problem and we propose a general prescription for calculating order parameters from simulations in systems with symmetry lower than uniaxial. We base our calculations on the simplest second rank attractive pair potential [3,10],

$$U(\omega_{ij}) = -\epsilon_{ij}\{P_2(\cos\beta_{ij}) + 2\lambda[R_{02}^2(\omega_{ij}) + R_{20}^2(\omega_{ij}) + 4\lambda^2 R_{22}^2(\omega_{ij})]\}, \quad (1)$$

with the biaxial molecules, or “spins,” fixed at the sites of a three-dimensional cubic lattice. The coupling parameter

$\epsilon_{ij}$  is taken to be a positive constant  $\epsilon$  when particles  $i$  and  $j$  are nearest neighbors and zero otherwise.  $\omega_{ij}$  is the Euler orientation of the molecular pair, given by three Euler angles  $\alpha$ ,  $\beta$ , and  $\gamma$  [18].  $P_2$  is a second Legendre polynomial and  $R_{mn}^L$  are combinations of Wigner functions  $D_{mn}^L$  [18] symmetry-adapted for the  $D_{2h}$  group of the two particles. Their explicit expressions, for the even terms, are

$$R_{mn}^L \equiv \frac{1}{2} \text{Re}(D_{mn}^L + D_{m-n}^L). \quad (2)$$

The biaxiality parameter  $\lambda$  accounts for the deviation from cylindrical molecular symmetry: when  $\lambda$  is zero, the potential Eq. (1) reduces to the well-known Lebwohl-Lasher  $P_2$  potential [19], while for  $\lambda$  different from zero the particles tend to align not only their major axis, but also their faces. The value  $\lambda = 1/\sqrt{6}$  marks the boundary between a system of prolate ( $\lambda < 1/\sqrt{6}$ ) and oblate molecules ( $\lambda > 1/\sqrt{6}$ ) and is analogous to the *self-dual* case described by Straley [2]. Thermodynamic results for a prolate particle at biaxiality  $\lambda$  and  $T^* \equiv kT/\epsilon$  can be mapped onto  $(\lambda', T^*) = [(3 - \lambda\sqrt{6})/(\sqrt{6} + 6\lambda)], 24T^*/(6\lambda + \sqrt{6})^2$  for the dual oblate particle.

We have performed Monte Carlo (MC) simulations [19] for 16 values of the biaxiality parameter  $\lambda$ , both on an  $8 \times 8 \times 8$  and a  $10 \times 10 \times 10$  lattice. For each  $\lambda$  value, about 40 temperatures have been investigated. For  $\lambda = 0.3$  additional larger size simulations ( $40 \times 40 \times 40$ ) have been performed at selected temperatures near the biaxial-nematic and nematic-isotropic transitions to rule out system size artifacts. The Metropolis MC method with periodic boundary conditions and controlled angular displacement [19,20] has been employed for lattice updates. We have typically used 30 000 lattice sweeps (cycles) for equilibration and 20 000 for production. The  $40 \times 40 \times 40$  system has required 40 and 30 kcycles. In Fig. 1 we show the heat capacity  $C_V$  obtained by differentiating the energy against temperature as described in [20] and plotted against temperature for  $\lambda = 0.2, 0.3$ , and  $0.40825$ . Starting with the lower values of  $\lambda$ , we see that  $C_V$  exhibits a small peak at low temperature

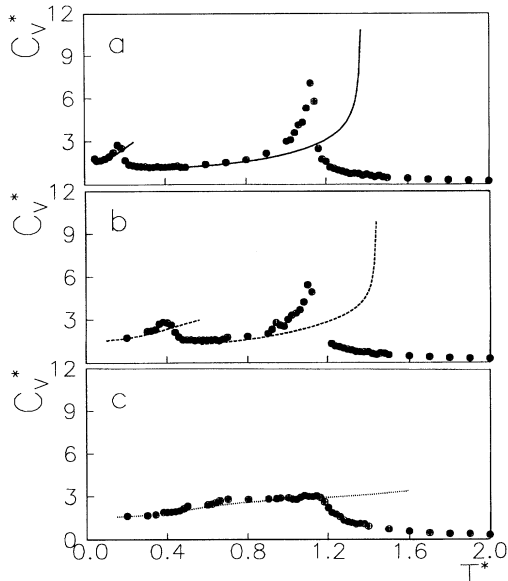


FIG. 1. Heat capacity  $C_V^* = C_V/k$  vs reduced temperature  $T^* \equiv kT/\epsilon$  for biaxiality  $\lambda = 0.2$  (a),  $0.3$  (b), and  $0.40825$  (c).  $10 \times 10 \times 10$  MC results are shown as symbols and MFT as continuous, dashed, and dotted lines, respectively.

and a sharper one at higher temperature corresponding to biaxial-uniaxial and uniaxial-isotropic phase transitions, respectively. The first transition shifts at higher temperature as  $\lambda$  increases, until the two peaks coalesce into a single broad hump near the self-dual case [Fig. 1(c)]. The MC phase diagram shown in Fig. 2 has been obtained from the peaks in the heat capacity. We see good agreement with the single result at  $\lambda = 0.2$  of Ref. [10] that was obtained with 512 particles and a fcc lattice, after scaling to 6 nearest neighbors.

The comparison between MC and MFT results obtained here following the procedure in Refs. [3,21] shows a

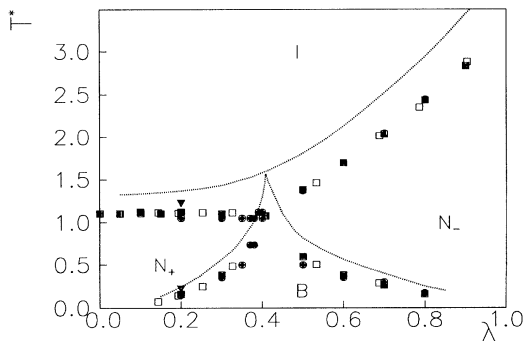


FIG. 2. Phase diagram showing the reduced transition temperature  $T^*$  vs  $\lambda$ . MC results are shown as filled squares ( $10 \times 10 \times 10$ ) and circles ( $8 \times 8 \times 8$ ). Empty squares are ( $10 \times 10 \times 10$ ) points mapped from  $(\lambda, T^*)$  onto  $(\lambda', T^{*'})$  (see text). MFT results are shown as continuous lines. The triangles at  $\lambda = 0.2$  are from Ref. [10].

rough qualitative agreement between the two methods. However, MFT predicts a rather pronounced increase with  $\lambda$ , while the simulations suggest an essentially constant transition temperature  $T_{N_+I}$ . Above the tricritical point, the transition temperature between  $N_-$  and the isotropic phase increases monotonically. We have used these points, where the variation in transition temperature is much greater than the error to generate the dual points below  $\lambda = 1/\sqrt{6}$ , marked as (+) in Fig. 2. We see that they confirm the small variation in  $T_{N_+I}$ . The MFT predictions worsen from a discrepancy of 17% to about 30% as the biaxiality increases and the transition becomes more second order.

We now turn to the determination of the order parameters and their temperature variation. In the principal axis system of a uniformly aligned biaxial phase the complete set of rank 2 order parameters consists of the averages  $\langle P_2 \rangle$ ,  $\langle R_{02}^2 \rangle$ , nonvanishing also in the uniaxial phase, and  $\langle R_{20}^2 \rangle$ ,  $\langle R_{22}^2 \rangle$ , different from zero only in the biaxial phase. In the isotropic phase, all the order parameters are zero. In the absence of external fields, the location of the principal system is unknown and can fluctuate during the simulation and thus has to be determined using rotational invariants for each configuration. For uniaxial systems this determination is usually realized by diagonalization of a suitable ordering matrix whose largest eigenvalue is the instantaneous order parameter and then averaging results for the various configurations. The calculation of biaxial order parameters is more complicated because of the need of a suitable prescription for assigning the two lower eigenvalues in a way that does not unduly enhance or cancel the phase biaxiality. We have attacked the problem using an approach similar to that of an actual experiment. We start by considering the general expression for the eigenvalues of a tensor property  $\mathbf{A}$  of a biaxial molecule, in the (principal) frame of a biaxial phase in terms of order parameters [22]:

$$a_{xx} = -\frac{1}{\sqrt{3}} A^{0,0} - \frac{1}{\sqrt{6}} (\langle P_2 \rangle A_{\text{MOL}}^{2,0} + 2\langle R_{02}^2 \rangle A_{\text{MOL}}^{2,2}) + (\langle R_{20}^2 \rangle A_{\text{MOL}}^{2,0} + 2\langle R_{22}^2 \rangle A_{\text{MOL}}^{2,2}), \quad (3)$$

$$a_{yy} = -\frac{1}{\sqrt{3}} A^{0,0} - \frac{1}{\sqrt{6}} (\langle P_2 \rangle A_{\text{MOL}}^{2,0} + 2\langle R_{02}^2 \rangle A_{\text{MOL}}^{2,2}) - (\langle R_{20}^2 \rangle A_{\text{MOL}}^{2,0} + 2\langle R_{22}^2 \rangle A_{\text{MOL}}^{2,2}), \quad (4)$$

$$a_{zz} = -\frac{1}{\sqrt{3}} A^{0,0} + \sqrt{\frac{2}{3}} (\langle P_2 \rangle A_{\text{MOL}}^{2,0} + 2\langle R_{02}^2 \rangle A_{\text{MOL}}^{2,2}), \quad (5)$$

where we use lowercase to indicate the eigenvalues, and  $A_{\text{MOL}}^{L,m}$  are irreducible spherical components of  $A_{\text{MOL}}$  of rank  $L$ . The order parameters are  $\langle P_2 \rangle = \langle R_{0,0}^2 \rangle = \frac{3}{2} \langle \cos^2 \beta \rangle - \frac{1}{2}$ ,  $\langle R_{02}^2 \rangle = \sqrt{3/8} \langle \sin^2 \beta \cos 2\gamma \rangle$ ,  $\langle R_{20}^2 \rangle = \sqrt{3/8} \langle \sin^2 \beta \cos 2\alpha \rangle$ , and  $\langle R_{22}^2 \rangle = \langle \frac{1}{4} (\cos^2 \beta + 1) \cos 2\alpha \cos 2\gamma - \frac{1}{2} \cos \beta \sin 2\alpha \sin 2\gamma \rangle$ .

Experimentally one would try to select a sufficient number of molecular properties  $A_{ij}^{\text{MOL}}$  and measure their average values  $\langle A_{ij}^{\text{LAB}} \rangle$ . Then, through a diagonalization of these average tensors  $\langle \mathbf{A}^{\text{LAB}} \rangle$  one could determine the order parameters. The requirement that these order parameters are the same for different observables helps in assigning the correct principal laboratory frame. As an illustration the explicit expressions for the eigenvalues of a tensor  $F_{ab} = \delta_{az}\delta_{bz}$  are

$$f_{XX} = \frac{1}{3} - \frac{1}{3} \langle P_2 \rangle + \sqrt{\frac{2}{3}} \langle R_{20}^2 \rangle, \quad (6)$$

$$f_{YY} = \frac{1}{3} - \frac{1}{3} \langle P_2 \rangle - \sqrt{\frac{2}{3}} \langle R_{20}^2 \rangle, \quad (7)$$

$$f_{ZZ} = \frac{1}{3} + \frac{2}{3} \langle P_2 \rangle. \quad (8)$$

The nontrivial problem is finding a consistent way of assigning the three eigenvalues  $f_1, f_2, f_3$  of the matrix  $\mathbf{F}$  to the  $X, Y, Z$  axes. In the uniaxial phase or any way when  $\langle R_{20}^2 \rangle \approx 0$ , and taking  $\langle P_2 \rangle > 0$ , we have  $f_{ZZ} > f_{XX} \approx f_{YY}$  and letting  $f_{ZZ} = \max(f_1, f_2, f_3)$  is sufficient to assign the axes except for an irrelevant exchange of  $X$  and  $Y$ . However, in the biaxial phase it may well happen that  $f_{XX} > f_{ZZ}$ , e.g., when  $\langle P_2 \rangle / \langle R_{20}^2 \rangle < \sqrt{2/3}$ , and, even if we assume that  $\langle P_2 \rangle$  and  $\langle R_{20}^2 \rangle$  are always positive, there is not a unique choice of axes other than assigning  $Y$  using  $f_{YY} = \min(f_1, f_2, f_3)$ . In particular, the basic assumption used to calculate  $\langle P_2 \rangle$  in the uniaxial case, i.e.,  $\max(f_1, f_2, f_3) = f_{ZZ}$ , breaks down. Fortunately in simulations we can perform more virtual experiments, determining the average of other probe properties sensitive to the alignment of the two other molecular axes. In practice, equations containing  $\langle R_{02}^2 \rangle$  and  $\langle R_{22}^2 \rangle$  as well as  $\langle P_2 \rangle$ ,  $\langle R_{20}^2 \rangle$  are constructed from the average of two other matrices, say  $G_{ab} = \delta_{ax}\delta_{bx}$  and  $H_{ab} = \delta_{ay}\delta_{by}$  by means of Eqs. (3)–(5). The resulting expressions of the order parameters in terms of the average tensors read

$$\langle P_2 \rangle = \frac{3}{2} f_{ZZ} - \frac{1}{2} \quad (9)$$

$$= 1 - \frac{3}{2} (g_{ZZ} + h_{ZZ}), \quad (10)$$

$$\langle R_{20}^2 \rangle = \sqrt{\frac{3}{8}} (f_{XX} - f_{YY}) \quad (11)$$

$$= \sqrt{\frac{3}{8}} (g_{YY} - g_{XX} + h_{YY} - h_{XX}), \quad (12)$$

$$\langle R_{02}^2 \rangle = \sqrt{\frac{3}{8}} (g_{ZZ} - h_{ZZ}) \quad (13)$$

$$= \sqrt{\frac{3}{8}} (h_{XX} + h_{YY} - g_{XX} - g_{YY}), \quad (14)$$

$$\langle R_{22}^2 \rangle = \frac{1}{2} (g_{XX} - g_{YY} + h_{YY} - h_{XX}). \quad (15)$$

The normalized eigenvectors of the matrices give the axes of the reference system, except for the sign, so there are

$3! = 6$  different systems corresponding to the eigenvalue permutations. We choose the eigenvalue permutation that satisfies the following conditions: (a)  $\langle P_2 \rangle > 0$ ; (b) the same order parameters must have the same values in all the ways they are computed (here, e.g.,  $\langle P_2 \rangle$  and  $\langle R_{20}^2 \rangle$  are computed in two different ways); (c) for each configuration at one temperature the order parameters must be as close as possible to the mean value of the order parameters of the previous temperature (the sum of the differences is minimized). The above procedure effectively assigns the  $X$  and  $Y$  axes when the phase is biaxial. In the uniaxial phase  $X$  and  $Y$  are undistinguishable and the method, even though not needed, is not applicable because it forces a difference that is completely spurious. In a similar way, application of the usual algorithm for finding  $\langle P_2 \rangle$  to an isotropic phase will give a spurious nonzero order parameter (decreasing with size).

The curves for  $\langle P_2 \rangle$  [Fig. 3(a)] exhibit the usual regular decrease with temperature and show no indication of the biaxial-uniaxial transition. While at low biaxiality the nematic-isotropic transition is sharp (although it appears continuous for these system sizes); the curve at  $\lambda = 0.40825$  shows a smooth decay consistent with the expected second order character of the transition. On the other hand, the molecular biaxiality parameter  $\langle R_{02}^2 \rangle$  [Fig. 3(b)] has a local maximum at the biaxial-uniaxial phase transition, is nonzero also in the uniaxial phase [2], and it increases with temperature until it reaches a maximum just below the nematic-isotropic transition. This behavior is qualitatively consistent with the MFT predictions.

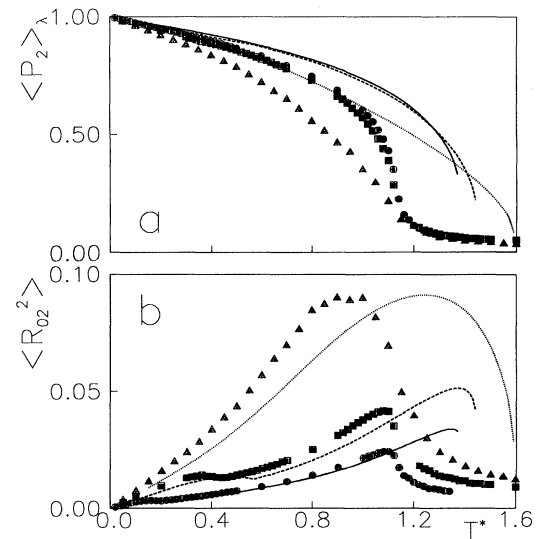


FIG. 3. Second rank order parameters vs  $T^*$ :  $\langle P_2 \rangle$  (a),  $\langle R_{02}^2 \rangle$  (b) obtained from  $10 \times 10 \times 10$  MC for  $\lambda = 0.2$  (circles),  $0.3$  (squares), and  $0.40825$  (triangles) together with MFT results (lines as in Fig. 1).

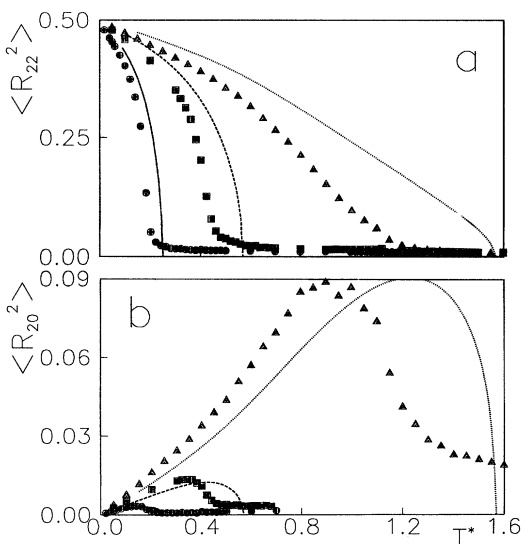


FIG. 4. Biaxial second rank order parameters vs  $T^*$ :  $\langle R_{22}^2 \rangle$  (a),  $\langle R_{20}^2 \rangle$  (b).  $10 \times 10 \times 10$  MC results for  $\lambda = 0.2$  (circles),  $0.3$  (squares), and  $0.40825$  (triangles). MFT results are shown as lines (cf. Fig. 1.)

In Fig. 4 the phase biaxiality parameters  $\langle R_{20}^2 \rangle$ ,  $\langle R_{22}^2 \rangle$  are shown. The order parameter  $\langle R_{22}^2 \rangle$  [Fig. 4(a)] decays monotonically from  $1/2$  to zero at the uniaxial phase transition. Because of this large variation (an order of magnitude larger than  $\langle R_{20}^2 \rangle$ ) this order parameter provides an effective monitor of the biaxial transition. The other parameter  $\langle R_{20}^2 \rangle$  is rather small, increases to a maximum value ( $<0.1$ ), and then decays smoothly to zero at the uniaxial phase transition.

It is worth noting that the quadrupolar asymmetry parameter that determines the observation of biaxial effects in deuterium NMR experiments [22] is estimated to be  $\eta = \sqrt{6} \langle D_{20}^2 \rangle / \langle P_2 \rangle$ . For a uniaxial probe  $\eta = 0.5$  when  $\lambda = 1/\sqrt{6}$  but for the other values  $\lambda = 0.2, 0.3$  is at the border of the threshold needed for NMR detection [16] ( $\eta \approx 0.2$ ). It seems that an important probe of phase biaxiality would instead be the measurement of  $\langle R_{22}^2 \rangle$ , possibly by the use of suitable biaxial, rather than uniaxial probes.

We are grateful to MURST, CNR. We thank the EU, HCM project, for partial support and Professor G. R. Luckhurst (Southampton) for useful discussions.

\*Present address: Istituto di Spettroscopia Molecolare and LAMEL-CNR, Bologna, Italy.

- [1] M. J. Freiser, Phys. Rev. Lett. **24**, 1041 (1970).
- [2] J. P. Straley, Phys. Rev. A **10**, 1881 (1974).
- [3] G. R. Luckhurst, C. Zannoni, P. L. Nordio, and U. Segre, Mol. Phys. **30**, 1345 (1975).
- [4] D. K. Remler and A. D. J. Haymet, J. Phys. Chem. **90**, 5426 (1986).
- [5] C. S. Shih and R. Alben, J. Chem. Phys. **57**, 3055 (1972); W. Li and K. F. Freed, J. Chem. Phys. **101**, 519 (1994).
- [6] D. W. Allender and M. A. Lee, Mol. Cryst. Liq. Cryst. **110**, 331 (1984).
- [7] E. F. Gramsbergen, L. Longa, and W. H. de Jeu, Phys. Rep. **135**, 195 (1986).
- [8] B. M. Mulder, Liq. Cryst. **1**, 539 (1986).
- [9] R. Holyst and A. Ponierewski, Mol. Phys. **69**, 193 (1990).
- [10] G. R. Luckhurst and S. Romano, Mol. Phys. **40**, 129 (1980); R. Hashim, G. R. Luckhurst, and S. Romano, Mol. Phys. **53**, 1535 (1984); R. Hashim, G. R. Luckhurst, F. Prata, and S. Romano, Liq. Cryst. **15**, 283 (1993).
- [11] C. D. Mukherjee and N. Chatterjee, Phys. Lett. A **189**, 86 (1994).
- [12] M. P. Allen, Liq. Cryst. **8**, 499 (1990).
- [13] L. J. Yu and A. Saupe, Phys. Rev. Lett. **45**, 1000 (1980).
- [14] F. Hessel and H. Finkelmann, Polymer Bull. **15**, 349 (1986).
- [15] S. Chandrasekhar, Contemp. Phys. **29**, 527 (1988); J. Malthête, L. Liébert, A. M. Levelut, and Y. Galerne, C. R. Acad. Sci. Paris **303**, 1073 (1986); K. Praefcke, B. Kohne, B. Gündoğan, D. Singer, D. Demus, S. Diele, G. Pelzl, and U. Bakow, Mol. Cryst. Liq. Cryst. **198**, 393 (1991); J-F. Li, V. Percec, C. Rosenblatt, and O. D. Lavrentovich, Europhys. Lett. **25**, 199 (1994).
- [16] S. M. Fan, I. D. Fletcher, B. Gündoğan, N. J. Heaton, G. Kothe, G. R. Luckhurst, and K. Praefcke, Chem. Phys. Lett. **204**, 517 (1993).
- [17] E. Berggren, R. Tarroni, and C. Zannoni, J. Chem. Phys. **99**, 6180 (1993); E. Berggren and C. Zannoni, Mol. Phys. (to be published).
- [18] M. E. Rose, *Elementary Theory of Angular Momentum* (Wiley, New York, 1957).
- [19] P. A. Lebowitz and G. Lasher, Phys. Rev. A **6**, 426 (1972); U. Fabbri and C. Zannoni, Mol. Phys. **58**, 763 (1986).
- [20] C. Chiccoli, P. Pasini, and C. Zannoni, Liq. Cryst. **2**, 39 (1987).
- [21] F. Biscarini, C. Zannoni, C. Chiccoli, and P. Pasini, Mol. Phys. **73**, 439 (1991).
- [22] C. Zannoni, in *The Molecular Dynamics of Liquid Crystals*, edited by G. R. Luckhurst and C. A. Veracini (Kluwer Academic Press, Dordrecht, 1994), Chap. 1.